Quintet and Septet State Systems Based on Pyridylnitrenes: Effects of Substitution on Open-Shell High-Spin States

ARTICLE *in* JOURNAL OF THE AMERICAN CHEMICAL SOCIETY · MARCH 2000

Impact Factor: 12.11 · DOI: 10.1021/ja993131c

4 AUTHORS, INCLUDING:

Sergei Victorovich Chapyshev
Russian Academy of Sciences
119 PUBLICATIONS **834** CITATIONS
SEE PROFILE

Paul Lahti
University of Massachusetts Amherst
253 PUBLICATIONS **3,443** CITATIONS
SEE PROFILE

Quintet and Septet State Systems Based on Pyridylnitrenes: Effects of Substitution on Open-Shell High-Spin States

Sergei V. Chapyshev,*,† Richard Walton,‡ Jon A. Sanborn,‡ and Paul M. Lahti*,‡

Contribution from the Institute for Chemical Physics, Chernogolovka, Russia, and the Department of Chemistry, University of Massachusetts, Amherst, Massachusetts 01003-4510

Received August 30, 1999

Abstract: Cryogenic matrix photolysis of 3,5-dichloro-2,4,6-triazidopyridine, 3-chloro-5-cyano-2,4,6-triazidopyridine, 3,5-dicyano-2,4,6-triazidopyridine, and 3,5-difluoro-2,4,6-triazidopyridine (**1**−**4**) gives rise to ESR spectral peaks of various triplet mononitrene, quintet dinitrene, and septet trinitrene species. The quintet 2,4-dinitrenes derived from **1**−**2** and **4** have zero-field splittings (zfs) of $|D/hc| \sim 0.22-0.24$ cm^{-1}, similar to values observed elsewhere for *m*-phenylene dinitrenes. 3,5-Dicyano-2,4,6-triazidopyridine (**3**) photolysis gives only a weak ESR signal corresponding to a mononitrene with a zfs of $|D/hc| \sim 1.22$ cm^{-1}. The spectrum from **1** also shows a 2,6-dinitrene with $|D/hc| = 0.283$ cm^{-1}, $|E/hc| = 0.036$ cm^{-1}, which illustrates the effects of heteroatom perturbation upon the zfs of a geometrically rigid *m*-arylene dinitrene. Spectral peaks for unusual septet 2,4,6-trinitrenopyridines derived from complete deazetation of **1**−**2** were also identified by simulation of the septet spectra. The zfs parameters for the trinitrenes were estimated to be $|D/hc| \sim 0.1$ cm^{-1}, with small *E*-values in both cases. Experimental and computational results support high spin ground states for the dinitrene and trinitrene species.

Introduction

In recent years there has been considerable progress in the study of high-spin polynitrenes as models for molecular electronic behavior.[1] Some key facts concerning these compounds remain unclear due to the complexity of aryl azide photochemistry. Because of the facile rearrangement of ortho-unsubstituted arylnitrenes to azaheptatetraenes[2] the yield of quintet dinitrenes under matrix photolysis conditions is uncertain. Intermediate azidonitrenes can be unstable to strong irradiation conditions and decompose into products of low molecular weight. But, mild irradiation of the same azidonitrenes may be insufficient for complete deazetation. Finally, some substituents could in principle influence the relative state energy ordering in polynitrenes, leading to low-spin ground states. As an example of the problems in polyazide photolysis, in 1966 Moriarty et al.[3] described cryogenic matrix photolysis of cyanuryl triazide, in which only a mononitrene signal was observed. Only recently has reinvestigation[1f] of the same reaction found ESR evidence for quintet state dinitrene products derived from deazetation of two out of the three azido groups.

Because of its complexity, the photochemistry of aryl azides has been subjected to considerable scrutiny.[4] Much less work has been devoted to the photochemistry of pyridyl azides.[5] Similarly, although considerable activity has been devoted to the study of electron−electron exchange effects of arenes bearing attached open-shell moieties, less effort has been devoted to use of corresponding heteroarenes such as pyridine. In one such study, Dougherty's group has shown that pyridine offers considerable flexibility as an electron exchange conduit, particularly through control of ground-state multiplicity by ring protonation.[6] Given the multiple possible exchange effects present in pyridine-based open-shell systems, we felt that it was worthwhile to investigate the pyridyl di- and trinitrenes. We are not aware of published reports of the ESR spectroscopy of such high-spin systems, which should offer much information about exchange interactions in small molecules having numerous unpaired electrons, and about the effects of heteroatom substitution on interactions between unpaired electrons.

In this article we describe ESR studies of products formed by photolysis of some 2,4,6-triazidopyridines[7−9] and the effects of substituents on the electronic properties of derived pyridyl di- and trinitrenes. The compounds studied were 3,5-dichloro-2,4,6-triazidopyridine, 3-chloro-5-cyano-2,4,6-triazidopyridine,

† Institute for Chemical Physics.

‡ University of Massachusetts.

(1) (a) Iwamura, H.; Murata, S. *Mol. Cryst. Liq. Cryst.* **1989**, *176*, 33. (b) Iwamura, H.; Nakamura, N.; Koga, N.; Sasaki, S. *Mol. Cryst. Liq. Cryst. Sci. Technol., Sect. A* **1992**, *218*, 207. (c) Buchachenko A. L. *Rus. Chem. Rev.* **1990**, *59*, 307 and references therein. (d) Lahti, P. M.; Minato, M.; Ling, C. *Mol. Cryst. Liq. Cryst.* **1995**, *271*, 147 and references therein. The zfs values suggested in this reference require reevaluation, in light of newer interpretations described in ref 13 below. (e) Ohana, T.; Kaise, M.; Nimura, S.; Kikuchi, O.; Yabe, A. *Chem. Lett.* **1993**, 765. (f) Nankai, T.; Sato, K.; Shiomi, D.; Takui, T.; Itoh, K.; Kozaki, M.; Okada, K. *Mol. Cryst. Liq. Cryst.* **1999**, *334*, 157. (g) Nimura, S.; Yabe, A. In *Molecular Magnetism of Organic Molecules and Materials*; Lahti, P. M., Ed.; Marcel Dekker: New York, 1999: pp 127−146.

(2) Wentrup, C. *Reactive Molecules. The Neutral Reactive Intermediates in Organic Chemistry*; Wiley-Interscience: New York, 1984; pp 212−221.

(3) Moriarty, R. M.; Rahman, M.; King, G. J. *J. Am. Chem. Soc.* **1966**, *88*, 842.

(4) (a) Lwowski, W. *Nitrenes*; Wiley-Interscience: New York, 1970. (b) Schuster, G. B.; Platz, M. S. *Adv. Photochem.* **1992**, *17*, 69. (c) Platz, M. S. *Acc. Chem. Res.* **1995**, *28*, 487. (d) Breslow, D. S. In *Azides and Nitrenes*; Scriven, E. F. U., Ed.; Academic: New York, 1984; p 491.

(5) (a) Evans, R. A.; Wong, M. W.; Wentrup, C. *J. Am. Chem. Soc.* **1996**, *118*, 4009 and citations in ref 7 therein. (b) Wentrup, C.; Kuzaj, M.; Lüerssen, H. *Angew. Chem., Int. Ed. Engl.* **1986**, *25*, 480.

(6) West, A. P., Jr.; Silverman, S. K.; Dougherty, D. A. *J. Am. Chem. Soc.* **1996**, *118*, 1452.

(7) Chapyshev, S. V. *Khim. Geterotsikl. Soedin.* **1993**, 1650. Chapyshev, S. V. *Chem. Heterocycl. Compd.*, **1993**, *29*, 1426.

(8) Chapyshev, S.V.; Bergstrasser, U.; Regitz, M. *Khim. Geterotsikl. Soedin.* **1996**, 67. Chapyshev, S.V.; Bergstrasser, U.; Regitz, M. *Chem. Heterocycl. Compd.* **1996**, *32*, 59.

(9) Chapyshev, S. V. *Khim. Geterotsikl. Soedin.* **1999**, 702.

10.1021/ja993131c CCC: $19.00
Published on Web 02/10/2000

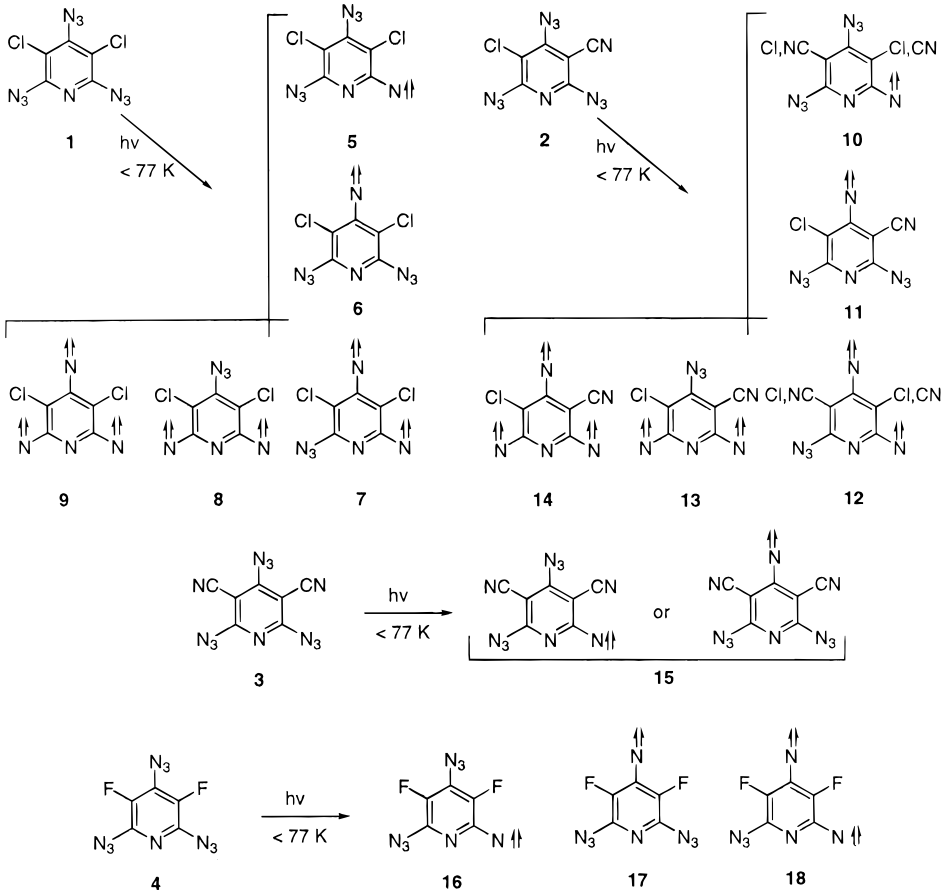

Figure 1. Products derived from cryogenic matrix photolysis of 2,4,6-triazdopyridines. Structure **12** could be a mixture of isomers.

3,5-dicyano-2,4,6-triazidopyridine, and 3,5-difluoro-2,4,6-triazidopyridine, **1**−**4** respectively (Figure 1). We describe the effects of heteroatom perturbation by the pyridine ring upon the ESR spectra of the product mononitrenes and dinitrenes. Further, we describe ESR spectral features derived from **1**−**2** that are attributable to septet state trinitrenes. To our knowledge, the quintet and septet spectral assignments and simulations given herein are the first for pyridine-based high-spin polynitrene systems.

Results

ESR Spectra from Triazides 1−**4**. Degassed samples of **1**−**4** in 2-methyltetrahydrofuran (2-MeTHF) were frozen at 77 K or below and photolyzed for 5 min through a Pyrex filter. Figures 2−5 show the X-band ESR spectra obtained from each sample, obtained at frequencies of 9.562, 9.560, 9.560, and 9.567 GHz, respectively. All spectra were stable to decomposition at 77 K for at least 1−2 h, but disappeared at once upon thawing of the matrix. Extended photolysis caused peak broadening and diminution of signal intensity in some cases, accompanied by an increase in the strength of the radical peak in the $g \sim 2$ region. Use of degassed, glassy ethanol as a solvent gave similar ESR spectra, except for variations in peak line shape.

The ESR spectral peaks can be assigned to mononitrene, dinitrene, and trinitrene species, save for the previously mentioned radical peak. Based on evidence that is discussed at length below, we find that triazide **1** yields intermediates **5**−**9**, triazide **2** yields **10**−**14**, triazide **3** yields **15**, and triazide **4** yields **16**−**18** (Figure 1). Peaks in the 6800−7500 G region are attributable to pyridyl mononitrenes, by analogy to previous work on related species.[5,10] Multiple peaks in the 100−3000 G region, as well as some peaks in the 3500−7000 G region, are attributable to quintet dinitrenes or septet trinitrenes. The quintet spectral features are comparable to those of other quintet dinitrenes, even though the ESR spectroscopy of pyridyl dinitrenes has not been described in the literature to our knowledge. As discussed below, some of the pyridyl dinitrenes show ESR spectral peak positions that are different from the expected positions, based on comparison to geometrically similar dinitrenes.[1] The differences are presumably due, at least in part, to heteroatom electronic perturbation.

Due to the importance of identifying peaks that belong to quintet dinitrene intermediates, as opposed to possible septet intermediates, we carried out simulations of putative quintet and septet portions of the appropriate spectra, using the eigenfield method described elsewhere.[11] The simulations are shown in the figures where appropriate.

Discussion

ESR Spectroscopy of 3,5-Dichloro-2,4,6-triazidopyridine (1) Photoproducts. The spectra obtained from photolysis of **1** were consistently stronger than those obtained from **2**−**4**. A strong monoradical peak at $g \sim 2$ arose from solvent photolysis and/or products of reaction between the nitrenes and the solvent. Two peaks were found in the mononitrene region (Figure 2a),

(10) Wasserman, E. *Prog. Phys. Org. Chem.* **1971**, *8*, 319.

(11) (a) Belford, G. G.; Belford, R. L.; Burkhalter, J. F. *J. Magn. Reson.* **1973**, *11*, 251. (b) Teki, Y.; Takui, T.; Yagi, H.; Itoh, K.; Iwamura, H. *J. Chem. Phys.* **1985**, *83*, 539. (c) Teki, Y.; Takui, T.; Itoh, K. *J. Chem. Phys.* **1988**, *88*, 6134. (d) Teki, Y.; Fujita, I.; Takui, T.; Kinoshita, T.; Itoh, K. *J. Am. Chem. Soc.* **1994**, *116*, 11499. (e) Teki Y. Ph.D. Thesis, Osaka City University, Osaka, Japan, 1985. (f) Sato, K., Ph.D. Thesis, Osaka City University, Osaka, Japan, 1994.

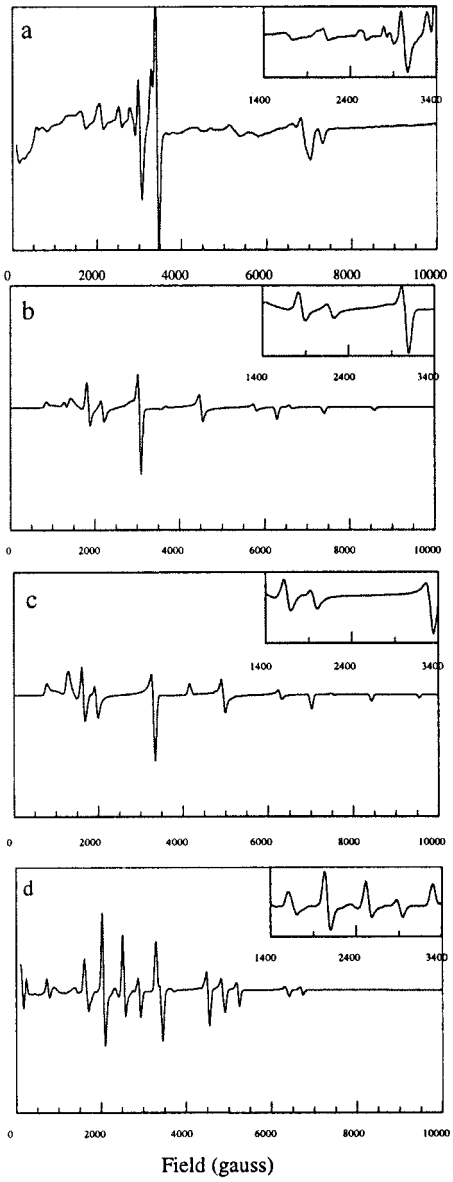

Figure 2. ESR spectroscopy of the photolyzate of **1**: (a) experimental spectrum (ν_0 = 9.562 GHz) at 77 K; (b) eigenfield simulation of a spectrum with $S = 2$, $g = 2.0030$, $D = 0.234$ cm^{-1}, $E = 0.031$ cm^{-1}; (c) eigenfield simulation of a spectrum with $S = 2$, $g = 2.0030$, $D = 0.283$ cm^{-1}, $E = 0.036$ cm^{-1}; and (d) eigenfield simulation of a spectrum with $S = 3$, $g = 2.0030$, $D = 0.100$ cm^{-1}, $E = 0.0005$ cm^{-1}.

consistent with the production of mononitrenes **5** and **6**. Eigenfield simulations[11f] yielded zfs values of $|D/hc| = 0.999$, $|E/hc| = 0.003$ cm^{-1} and $|D/hc| = 1.130$ cm^{-1}, $|E/hc| \sim 0.002$ cm^{-1} for **5** and **6**, respectively. We attribute the nitrene peak at lower field to 2-nitrenopyridine (**5**), and the higher field peak to 4-nitrenopyridine (**6**). Wentrup's group has found that electron acceptor substituted pyridyl-2-azides yielded mononitrenes with zfs of $|D/hc| = 1.05-1.10$ cm^{-1}.[5] The assignment of the 2- vs the 4-pyridinyl nitrenes is supported by comparison to ESR spectra derived from structurally similar molecules containing azide moieties in either the 2- or the 4-position, but not in both.[12]

Based upon the eigenfield spectral simulation shown in Figure 2b, we assigned the ESR features at 1670, 2120, and 3030 G to quintet state 2,4-dinitrene **7**. These features were satisfactorily

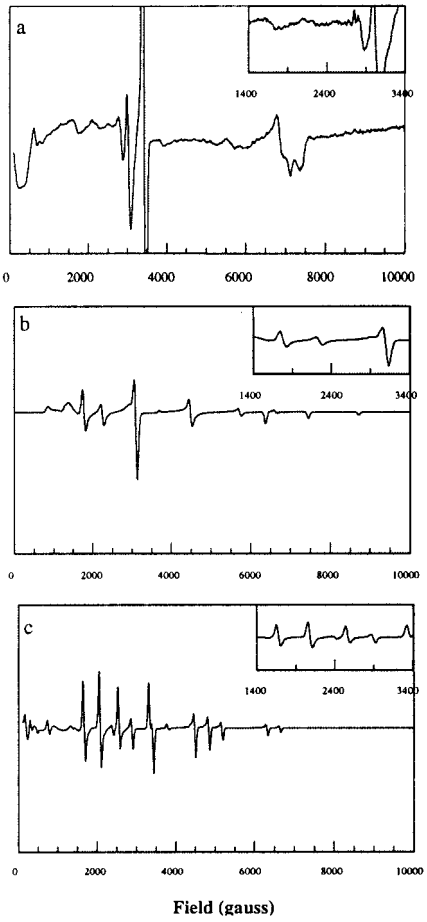

Figure 3. ESR spectroscopy of the photolyzate of **2**: (a) experimental spectrum (ν_0 = 9.560 GHz) at 77 K; (b) eigenfield simulation of a spectrum with $S = 2$, $g = 2.0030$, $D = 0.236$ cm^{-1}, $E = 0.033$ cm^{-1}; and (c) eigenfield simulation of a spectrum with $S = 3$, $g = 2.0030$, $D = 0.098$ cm^{-1}, $E = 0.000$ cm^{-1}.

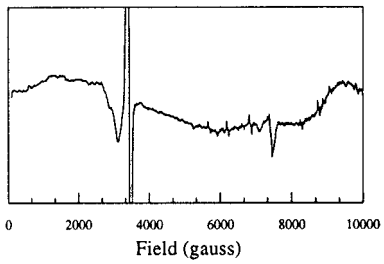

Figure 4. ESR spectroscopy of the photolyzate of **3** (experimental spectrum ν_0 = 9.560 GHz at 77 K).

reproduced by the following parameters: $S = 2$, $g = 2.003$, $|D/hc| = 0.234$ cm^{-1}, and $|E/hc| = 0.031$ cm^{-1}. These zfs parameters are quite similar to those recently determined to apply to other *m*-arylene dinitrenes, such as 5-nitro-1,3-phenylenedinitrene.[13] The effect of the pyridine nitrogen upon the zfs parameters of **7** appears minor, based upon the small change in the quintet spectrum relative to those of related *m*-arylene dinitrenes.

A prominent feature in the spectrum of Figure 2a was a partially resolved peak at about 3350 G at slightly lower field than the g ~ 2 radical impurity peak. We assigned this peak to the 2,6-pyridinedinitrene **8**. This is a novel ESR peak position

(12) (a) Chapyshev, S. V.; Walton, R.; Lahti, P. M. Unpublished observations. (b) Walton, R. Ph.D. Thesis, University of Massachusetts, Amherst, MA, 1998.

(13) Fukuzawa, T. A.; Sato, K.; Ichimura, A. S.; Kinoshita, T.; Takui, T.; Itoh, K.; Lahti, P. M. *Mol. Cryst. Liq. Cryst. Sci. Technol., Sect. A* **1996**, *278*, 253.

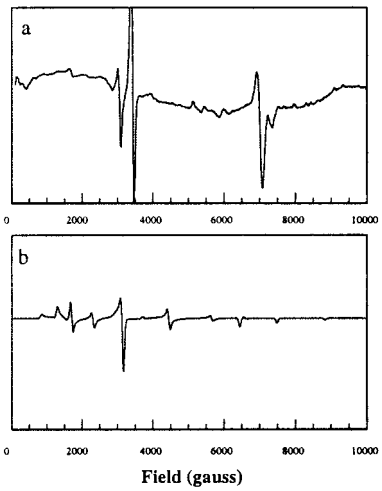

Figure 5. ESR spectroscopy of the photolyzate of **4**: (a) experimental spectrum ($\nu_0 = 9.567$ GHz) at 77 K and (b) eigenfield simulation of a spectrum with $S = 2$, $g = 2.0030$, $D = 0.237$ cm^{-1}, $E = 0.035$ cm^{-1}.

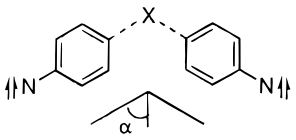

Figure 6. Schematic diagram of a quintet dinitrene composed of weakly interacting mononitrene sites with a known vector angle 2α formed by the two C−N bonds.

for a quintet dinitrene, since previously observed *m*-phenylene-dinitrenes all have their major peak at about 3000 ± 100 G, for reasons that will be described below. Figure 2c shows a simulation of the spectrum of **8** having the following parameters: $S = 2$, $g = 2.003$, $|D/hc| = 0.283$ cm^{-1}, and $|E/hc| = 0.036$ cm^{-1}. A number of the simulated features for 2,6-dinitrene **8** overlie or fall close to the features for 2,4-dinitrene **7**, except for the major peak of **8** at 3350 G. By themselves, these spectra do not prove that the spectral assignments of **7** and **8** are not reversed from those proposed. However, the similarity of the spectrum assigned to **7** to those previously seen[1b] for *m*-arylene dinitrenes compels the given assignments.

Heteroatom perturbation effects in high-spin zfs have not been tested much in dinitrene work. Itoh has shown that the zfs of quintet state systems composed of weakly interacting triplet sites will be largely determined by the dipolar interaction angle 2α between the two triplet sites (Figure 6), so long as the one-center interaction within the triplet sites is strong.[14] Dinitrenes are appropriate systems for application of the Itoh model. The full derivation and mathematical relationship between the experimental zfs parameters of the interacting triplet sites and the interaction angle is given elsewhere,[14] but a brief summary follows.

The dipolar relationship between quintet zfs and the triplet zfs of its component parts in Figure 6 follows eq 1

$$\mathbf{D}_{\mathrm{Q}}{}^{S=2} = \frac{1}{6}(\mathbf{D}_1{}^{S=1} + \mathbf{D}_2{}^{S=1}) + \frac{1}{3}\mathbf{D}_{12} \qquad (1)$$

where $\mathbf{D}_{\mathrm{Q}}$ is the zfs tensor for the overall quintet state, $\mathbf{D}_1$ and $\mathbf{D}_2$ are the zfs tensors for the interacting triplet centers, and $\mathbf{D}_{12}$ is the tensor element representing interaction between the two centers. Assuming that the one-center interactions dominate, the cross term can be ignored ($\mathbf{D}_1$, $\mathbf{D}_2 \gg \mathbf{D}_{12}$), leading to eq 2

$$D_{\mathrm{aa}} = \frac{1}{3}\left(-(\mathrm{D}_t + \mathrm{E}_t)\sin^2\alpha + \frac{2}{3}D_{\mathrm{t}}\right)$$

$$D_{\mathrm{bb}} = \frac{1}{3}\left((D_{\mathrm{t}} + E_{\mathrm{t}})\sin^2\alpha - \left(\frac{D_{\mathrm{t}}}{3} + E_{\mathrm{t}}\right)\right)$$

$$D_{\mathrm{cc}} = \frac{1}{3}\left(-\frac{D_{\mathrm{t}}}{3} + E_{\mathrm{t}}\right) \qquad (2)$$

which relates the diagonal elements D_{aa}, D_{bb}, and D_{cc} of the quintet zfs tensor to the zfs *D*- and *E*-values of the triplet centers, D_{t} and E_{t}. With appropriate assignment of axes in Figure 5, $D_{\mathrm{aa}} = D_{\mathrm{zz}}$, where D_{zz} is the zz tensor element of $\mathbf{D}_{\mathrm{Q}}$, eq 3 can be derived from eq 2 to relate the quintet zfs spectral parameters D_{Q} and E_{Q} to D_{zz}, and hence to angle α between the C−N bonds of the dinitrene (see Figure 6).

$$D_{\mathrm{Q}} = \frac{3}{2}D_{\mathrm{ZZ}}{}^{S=2}$$

$$E_{\mathrm{Q}} = \frac{1}{2}(D_{\mathrm{XX}}{}^{S=2} - D_{\mathrm{YY}}{}^{S=2}) \qquad (3)$$

Kalgutkar and Lahti have shown[15] that Itoh's model successfully describes the zfs behavior of geometrically constrained quintet dinitrenes **19**−**21**. Since a large number of aryl dinitrenes composed of interacting phenylnitrene units with $2\alpha \sim 120°$ all have quintet ESR spectra with a major peak at about 3000 G,[1d] one presumes that any aryl dinitrene with molecular geometry $2\alpha \sim 120°$ will have such a spectrum, including the 2,4-pyridine dinitrenes **7**, **12**, and **18** in Figure 1.

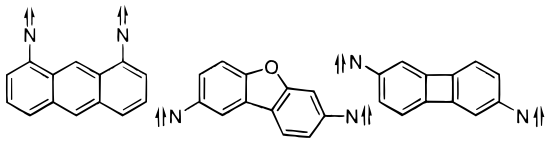

19 **20** **21**

By Itoh's model, 2,4-dinitrene **7** is predicted to have $|D_{\mathrm{Q}}/hc| = 0.223$ cm^{-1} and $|E/hc| = 0.044$ cm^{-1}, applying eqs 2−3 with the observed triplet mononitrene zfs values from Figure 2 of $|D_t/hc| = 0.999$ and 1.130 cm^{-1}, and assuming angle $2\alpha = 120°$. The predicted value compares well with the observed zfs parameters of $|D/hc| = 0.234$ cm^{-1} and $|E/hc| = 0.031$ cm^{-1}. 2,6-Dinitrene **8** is predicted by the same procedure to have $|D_{\mathrm{Q}}/hc| = 0.185$ cm^{-1} and $|E/hc| = 0.049$ cm^{-1}, using the assigned zfs value of 0.999 cm^{-1} for 2-nitrene **5** with $2\alpha = 114°$ (based on computations described below for a model 2,6-pyridine dinitrene). This predicted *D*-value is much smaller than the observed $|D/hc| = 0.283$ cm^{-1} assigned to **8**. If one uses the high-field nitrene zfs value of 1.13 cm^{-1} from the photolysis ESR spectrum of **1**, and 2α values of 114° and 120°, the predicted values of $|D_{\mathrm{Q}}/hc|$ are still only 0.209 and 0.235 cm^{-1}. We presume that the difference between the predicted and observed spectral zfs for **8** is due to heteroatom perturbation of spin density distribution. Further support for the assignment of the 3350 G spectral feature of Figure 2a to 2,6-dinitrene **8** is given by experiments that show formation of a characteristic

(14) Itoh, K. *Pure Appl. Chem.* **1978**, *50*, 1251.

(15) (a) Kalgutkar, R. S. Ph.D. Thesis, University of Massachusetts, Amherst, MA, 1998. For dinitrene **21**, the experimental zfs are $|D/hc| = 0.260$ cm^{-1} and $|E/hc| < 0.0005$ cm^{-1}. (b) Kalgutkar, R. S.; Lahti, P. M. *J. Am. Chem. Soc.* **1997**, *119*, 4771−4772.

ESR peak at about 3300−3400 G when other 2,6-diazidopyridine derivatives are photolyzed under cryogenic conditions.[12]

After assigning ESR peaks in Figure 2a as described above, a set of peaks remains unassigned in the 2400−2900 and the 5000−6000 G regions. These peaks were not formed when triazide **1** was photolyzed at 77 K with monochromatic 313 nm light for 10 min, but did appear when the frozen 313 nm photolyzate was photolyzed again with broadband light of >300 nm. The intensity of these peaks varied somewhat from experiment to experiment relative to the intensities of the peaks assigned in the preceding paragraphs, hence they are not portions of the dinitrene spectra. A variety of quintet simulations with reasonable *D*- and *E*-values likewise did not generate peaks in this region, further arguing against assigning these peaks to 2,4- or 2,6-dinitrene species. If quintet dinitrene species are ruled out, then a plausible carrier of these peaks is trinitrene **9**.

There is very little precedent for interpreting the ESR spectroscopy of systems with three nitrene units attached to a single conjugated ring system. Photolysis of 1,3,5-triazido-2,4,6-tricyanobenzene (**22)** was reported to yield an ESR spectrum attributed to 1,3,5-aryltrinitrene (**23**). That spectrum was not available to allow a comparison to the present results. In that experiment, Wasserman and co-workers[16] assigned ESR peaks at 420, 1650, and 2750 G to trinitrene **23** and estimated its zfs to be $|D/hc| = 0.0548 \pm 0.008$ cm^{-1}. The assignment was based on the absence of a signal at 8400 G that was deemed typical for quintet dinitrenes. At the time, there was very little experimental data concerning quintet dinitrene ESR spectra, hence comparison to other cases was not easy. As we shall explain below, the present study has an advantage of 30 subsequent years of ESR spectral studies of dinitrenes, making the assignment of ESR peaks more certain.

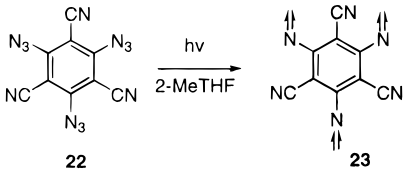

22 **23**

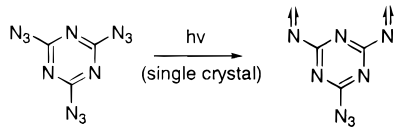

24 **25**

Photolysis of the geometrically related cyanuric triazide **24** was originally reported[3] to give an ESR spectrum with large mononitrene zfs ($|D/hc| = 1.44$ cm^{-1}); these workers suspected that the *s*-triazine ring fragmented in that experiment. No mention was made in that report of spectral peaks attributable to any higher multiplicity state. More recently, photolysis of **24** in a crystalline matrix was shown[4] to give a quintet ESR spectrum with $|D/hc| = 0.280$ cm^{-1} and $|E/hc| = 0.058$ cm^{-1}, presumably the dinitrene product **25** derived from double deazetation. The latter result is consistent with the zfs values that we attribute to 2,6-pyridinedinitrene (**8**), and further supports the structural assignment of this portion of the ESR spectrum that was described above. No ESR-detectable amount of trinitrene product appears to have been formed from **24**.

The spectrum of Figure 2a has a broad feature in the 100−600 G region, better-defined peaks at 1700, 2120, and 2560 G, and a double peak at about 2850 G. The low-field feature plus the features at 1700 and 2850 G correlate with peak positions described[16] by Wasserman and co-workers. To assist our assignments, we simulated septet ESR spectra by the eigenfield method. Using the parameters $S = 3$, $g = 2.003$, $|D/hc| = 0.100$ cm^{-1}, and $|E/hc| = 0.0005$ cm^{-1}, the spectrum shown in Figure 2d was obtained. The spectral appearance is very sensitive to minor changes in the *D*- and *E*- values used in the simulation, but gave peaks that are all close to those observed in the 2000−3000 G region, without giving strong peaks elsewhere in the spectrum. Some moderate intensity peaks in the 3500−5000 G region are seen in the simulation, which are broader in the experimental spectrum due to higher-order line shape effects. The simulated septet peaks at about 1700, 2100, and 3300 G overlap with peaks assigned to the quintets, consistent with the slightly broadened and distorted appearances of these peaks in the experimental spectrum. It may be that the 3300 G peak is due only to septet **9** rather than containing a component from 2,6-dinitrene **8**. However, we have routinely observed an ESR peak at 3300 G in the photolysis of 2,6-diazidopyridines that do not have 4-azido substituents,[12] so we feel that **8** is most likely present and is a contributor to the peak at 3300 G. Overall, a combination of the quintet and septet simulations in Figure 2b−d accounts very well for the peaks in the 1000−3400 G region of the experimental spectrum derived from triazide **1**.

The complexity of simulating the septet spectrum makes it difficult to prove unequivocally that the spectral features assigned to a septet are generated by trinitrene **9**. However, a logical outcome of exhaustive azide photolysis for **1** should be the formation of trinitrenes. Alternative carriers for these peaks are not obvious, given a lack of conformational isomers to produce variation[17] in the quintet spectral zfs. In addition, the simulations give a good account of spectral features assigned to the putative septets. The bulk of evidence is supportive of our assignments, and there are no contradictory data. In the preceding article in this journal by Wentrup and co-workers,[18] independent IR spectroscopic evidence is given that supports our assertion that intermediates **5**−**9** are formed in the photolyzate of **1**.

ESR Spectroscopy of 3-Chloro-5-cyano-2,4,6-triazidopyridine (2) Photoproducts. The mononitrene region 6800−7500 G in Figure 3 is more complex than that in Figure 2, consistent with the three possible mononitrenes (**10** and **11**) arising from azide photocleavage of **2**. This region is consistent with an overlay of three mononitrene peaks with zfs values of $|D/hc| = 1.000$, 1.006, and 1.115 cm^{-1}, assuming that all have small *E*-values in accord with typical aryl mononitrene spectra.[10]

Spectral features at 1700, 2200, and 3020 G are attributable to a quintet 2,4-dinitrene of type **12** by analogy to the analysis in the preceding section, and are satisfactorily reproduced by eigenfield spectral simulation using the following parameters: $S = 2$, $g = 2.003$, $|D/hc| = 0.236$ cm^{-1}, and $|E/hc| = 0.033$ cm^{-1}. There are two possible 2,4-dinitrenes **12**, and it is possible that both or either are present. No resolvable peak at about 3350−3400 G attributable to 2,6-dinitrene **13** was seen here. Such a peak might be present but obscured by $g \sim 2$ radical impurity absorption, but it is also possible that 2,6-dinitrene **13** is not formed in large amounts.

The overall intensity of peaks derived from **2** relative to the radical impurity peak is weaker than is found in the photolysis

(16) Wasserman, E.; Schueller, K.; Yager, W. A. *Chem. Phys. Lett*. **1968**, *2*, 259.

(17) (a) Nimura, S.; Kikuchi, O.; Ohana, T.; Yabe, A.; Maise, M. *Chem. Lett.* **1993**, 837−838. (b) Ling, C.; Lahti, P. M. *J. Am. Chem. Soc.* **1994**, *116*, 8784−8792.

(18) Chapyshev, S. V.; Kuhn, A.; Wong, M.; Wentrup, C. *J. Am. Chem. Soc*. **2000**, *122*, 1572−1579.

of **1**. We attribute the weakened intensity of the overall spectrum and apparent lack of a 2,6-dinitrene peak to the presence of the cyano group in **2** that is ortho to an azide group. As we shall note below, ortho cyano groups impede formation of ESR active nitrene sites.

After assigning ESR peaks in Figure 3a to mononitrenes and 2,4-dinitrene **12**, an ESR feature at ~2800 G remains that is quite similar to the one at ~2850 G in Figure 2a. Presumably this peak arises from septet **14**, applying the same logic used to argue in favor of **9**. Using $S = 3$, $g = 2.003$, $|D/hc| = 0.098$ cm^{-1}, and $|E/hc| = 0.000$ cm^{-1}, we obtained the eigenfield spectral simulation shown in Figure 3c. The simulated septet spectrum has a number of peak overlaps with quintet peaks, and the central septet peak is predicted to be overlaid by the experimental $g \sim 2$ line. Otherwise, the line positions predicted from the simulation are consistent with the experimental lines. Based on this evidence, photolysis of **2** also leads to formation of septet trinitrene species. IR spectral evidence based on matrix-isolated photolysis of **2** further supports the presence of mono-, di-, and trinitrene formation, as reported in the preceding article by Wentrup and co-workers.[18]

ESR Spectroscopy of 3,5-Dicyano-2,4,6-triazidopyridine (3) Photoproducts. The mononitrene region in Figure 4 is quite a bit weaker in intensity than in Figures 2 and 3. One peak is found at about 7400 G, corresponding to a zfs of $|D/hc| \sim 1.22$ cm^{-1}. This is the sole ESR spectral feature derived from **3**, although it is possible that a 2,6-dinitrene peak might be concealed by the $g \sim 2$ peak at 3400 G. The 3400 G peak itself is unlikely to be a 2,6-dinitrene peak, due to the lack of other peaks indicated by our quintet in Figures 2 and 3. The mononitrene could be formed by deazetation at the 2- or the 4-position, hence structure **15** is shown as either possibility. The large zfs is due to the electronic effect of the cyano group, which apparently increases the π-spin density on the nitrene nitrogen.

The cyano group also has a strong effect upon the photochemical behavior of the pyridyl triazides. As described in the previous section, the introduction of the cyano group in **2** caused the overall intensity of the spectrum to decrease when the photolysis was carried out under conditions similar to those used for **1**. Cyano- and fluoro-substituted arylnitrenes have a tendency to exhibit singlet state reactivity.[19] If this occurred in systems **3**−**4**, we might expect to get a higher percentage of singlet manifold rearrangements that would preclude observation of the ESR active open-shell states that retain the pyridine ring. We cannot say for certain what is occurring based upon ESR spectroscopy alone, but compound **3** exhibits essentially complete suppression of the high multiplicity peaks found in the photolyses of **1**−**2**. In the preceding article by Wentrup and co-workers,[18] IR spectroscopic investigations likewise found that nitrene production for **3** is inefficient relative to that in **1**−**2**; this is apparently due to a greater tendency for **3** to rearrange.

ESR Spectroscopy of 3,5-Difluoro-2,4,6-triazidopyridine (4) Photoproducts. The photolysis of **4** yielded the spectrum shown in Figure 5. Aside from the usual $g \sim 2$ peak, a major and a minor mononitrene peak were found with zfs values of $|D/hc| = 1.005$ and 1.113 cm^{-1}, respectively, which are assigned to mononitrenes **16**−**17** by the same arguments described above. A major peak was found at ~3000 G, corresponding to 2,4-dinitrene **18**. Eigenfield quintet simulation is consistent with quintet zfs of $|D/hc| = 0.237$ cm^{-1} and $|E/hc| = 0.035$ cm^{-1}. As was the case with the spectra in Figures 2 and 3, simulated spectral intensities are hard to match for the minor peaks, but the major peak positions are adequately matched. Applying eqs 2 and 3 as was done above, using *D*-values of 1.005 and 1.113 cm^{-1} for the 2- and 4-nitrene units, and assuming that $2\alpha = 120°$, the quintet zfs parameters of **18** are predicted to be $|D/hc| = 0.221$ cm^{-1} and $|E/hc| = 0.044$ cm^{-1}, in good agreement with the observed values.

No resolved 2,6-dinitrene peak was experimentally observed in the 3300−3400 G region, nor were there any major peaks attributable to septet species. Apparently the septet derivable from **4** is not formed under these conditions, is not stable, or is not a thermally populated state. Using the assignments described above, the ESR spectrum shows predominant initial cleavage of the 2-azido group in **4**, followed by some cleavage of the 4-azido group to give quintet **18**. Assuming that there is no inherent stability in a trinitrene derived from **4**, it appears that photolysis of all three azido groups in **4** is an inefficient process.

Ground States of Dinitrenes and Trinitrenes. All of the meta dinitrenes and 2,4,6-trinitrenes shown in Figures 1−5 are expected to have high-spin ground states based on spin parity arguments. We checked the ESR doubly integrated signal intensities as functions of reciprocal absolute temperature ($1/T$) over a 4−65 K temperature range. All of the peaks in the 1500−3100 G range in Figure 2a showed essentially linear intensity behavior with $1/T$, in obedience to the Curie law, and as expected if the signal carriers are ground states by at least 1 kcal/mol. The intensity variation was reversible when the temperature was raised and then lowered, showing that sample decomposition did not occur over the lifetime of the Curie law experiment. The 3350 G signal from dinitrene **8** lies on the shoulder of the $g \sim 2$ peak, but its signal intensity was monitored in terms of peak height above the baseline of the spectrum, and it also showed linear Curie law behavior.

There is a formal possibility that any or all of the quintet and septet state species in Figure 1 are virtually degenerate with other states, a situation that would also yield a linear Curie plot.[20] We considered this unlikely, given the strong quintet state preference in ab initio computations for meta-conjugated systems of this type. Ichimura et al.[21] found that the quintet state in *m*-phenylenedinitrene is a ground state by at least 4−6 kcal/mol relative to the corresponding triplet state, using SCF-configuration interaction computations with a split valence plus polarization basis set. Dougherty and co-workers[6] carried out computations on open-shell systems in which radical sites were linked by pyridine units with meta connectivity. They found 2,6-dimethylenepyridine to favor a high spin ground state by 8.4 kcal/mol, indicating that neutral 2,6-pyridinediyl acts qualitatively like *m*-phenylene. Experimental studies by these workers confirmed this prediction.

We believed that the 2,4-dinitrene quintets **7**, **12**, and **18** should not exhibit greatly altered exchange behavior by comparison to the closely related *m*-phenylenedinitrene. However, we were concerned lest 2,6-dinitrenes **8** and **13** show different quintet−triplet energy splitting, in the same manner that 2,6-dinitrene **8** shows different zfs splitting from the 2,4-dinitrenes. We therefore carried out ab initio complete active space self-consistent field (CASSCF) post-Hartree−Fock geometry optimization on the lowest quintet and triplet states for

(19) (a) Dunkin, I. R.; Donnellyu, T.; Lockhart, T. S. *Tetrahedron Lett.* **1985**, *26*, 359. (b) Poe, R.; Schnapp, K.; Young, M. J. T.; Grayzar, J.; Platz, M. S. *J. Am. Chem. Soc.* **1992**, *114*, 5054. (c) Marcinek A.; Platz M. S.; Chan, S. Y.; Floresca, R.; Rajagopalan, K.; Golinski, M.; Watt, D. *J. Phys. Chem.* **1994**, *98*, 412. (d) Michalak J.; Zhai, H. B.; Platz, M. S. *J. Phys. Chem.* **1996**, *100*, 14028.

(20) For a discussion of the limitations of Curie law analysis, see: Berson, J. A. In *The Chemistry of Quinoid Compounds*; Patai, S., Rappaport, Z., Eds.; Wiley: New York, 1988;Vol. 2, pp 462−469.

(21) Ichimura, A. S.; Lahti, P. M. *Mol. Cryst. Liq. Cryst.* **1993**, *233*, 33−40.

parent 2,6-pyridinedinitrene (**26**) using an eight-orbital, eight-electron active space (CASSCF(8,8)) with the standard Pople-type 6-31G* basis set in the program[22] GAMESS. In addition, we carried out density functional theory (DFT) computations with the 6-31G* basis set using Gaussian 98.[23] Septet state computations were carried out using standard unrestricted hybrid B3LYP[24] functionals (UB3LYP), while quintet and triplet states for the dinitrenes and trinitrenes were carried out using the GUESS(MIX) keyword in Gaussian 98 to allow for symmetry-mixed wave functions. This approach has been useful in studying other open-shell systems, and we felt that a comparison of CASSCF and DFT methodologies in these high-spin species would be instructive.

Figure 7 shows selected geometric data and energies from these computations. Supporting material shows contour diagrams of the active space orbitals used in these computations, as well as various other data. The quintet reference state for **26** was $1a_2^2\ 10b_2^2\ 14a_1^1\ 2b_1^1\ 3b_1^1\ 2a_2^1\ 4b_1^0\ 3a_2^0$; all higher virtual orbitals and lower occupied orbitals were frozen. The CASSCF-(8,8)/6-31G*//CASSCF(8,8)/6-31G* energy of the $^5A_2$ state of **26** was −354.1673798 hartrees. The corresponding $^3A_1$ state energy for **26** was −354.1106730 hartrees, corresponding to a surprisingly large quintet−triplet energy gap of 36 kcal/mol. The DFT results showed a considerably smaller, but still sizable, quintet−triplet gap of 14 kcal/mol. Given these computational results, we feel that the likelihood of quintet−triplet near-degeneracy in the 2,6-pyridine dinitrenes is low, even allowing for sizable substituent effects.

We also carried out CASSCF and DFT geometry optimizations on the $^7A_2$ and $^5B_2$ states of parent trinitrenopyridine **27**, in a manner analogous to the computations for **26**. This active space included all three of the "lone pair" type, σ symmetry orbitals that contain unpaired, localized electrons on the nitrene sites, plus a set of three singly occupied, one doubly occupied, and one virtual π-orbitals. Diagrams of these active space orbitals are included in Supporting Information. Figure 7 shows selected CASSCF(8,8)/6-31G* geometric data and energies for these two computed states. These geometries were frozen, and the active space expanded to a CASSCF(10,10) set for a final set of computations, using the same basis set. The CASSCF-(10,10) active space $^7A_2$ reference configuration was $2b_1^2\ 1a_2^2\ 10b_2^1\ 16a_1^1\ 11b_2^1\ 3b_1^1\ 4b_1^1\ 2a_2^1\ 5b_1^0\ 3a_2^0$; all higher virtual orbitals and lower occupied orbitals were frozen. The same active space orbitals (with different occupancies) and computational procedures were used for the $^5B_2$ state. The CASSCF-(10,10)/6-31G*//CASSCF(8,8)/6-31G* energy for the $^7A_2$ state was −408.17960, while the corresponding energy for the $^5B_2$ state was −408.105971. This corresponds to a large septet−quintet energy gap of 46 kcal/mol. The $^7A_2$ state has two dominant configurations in the CASSCF(10,10) computation, occupancies 2111111200 and 2211111100 using the active space orbitals cited earlier in this paragraph. But, the $^5B_2$ state is highly mixed with numerous configurations having coefficients of >0.20. SCF-CISD computations with a 20 orbital active space indicated that the CASSCF(10,10) active space included all major configurations.

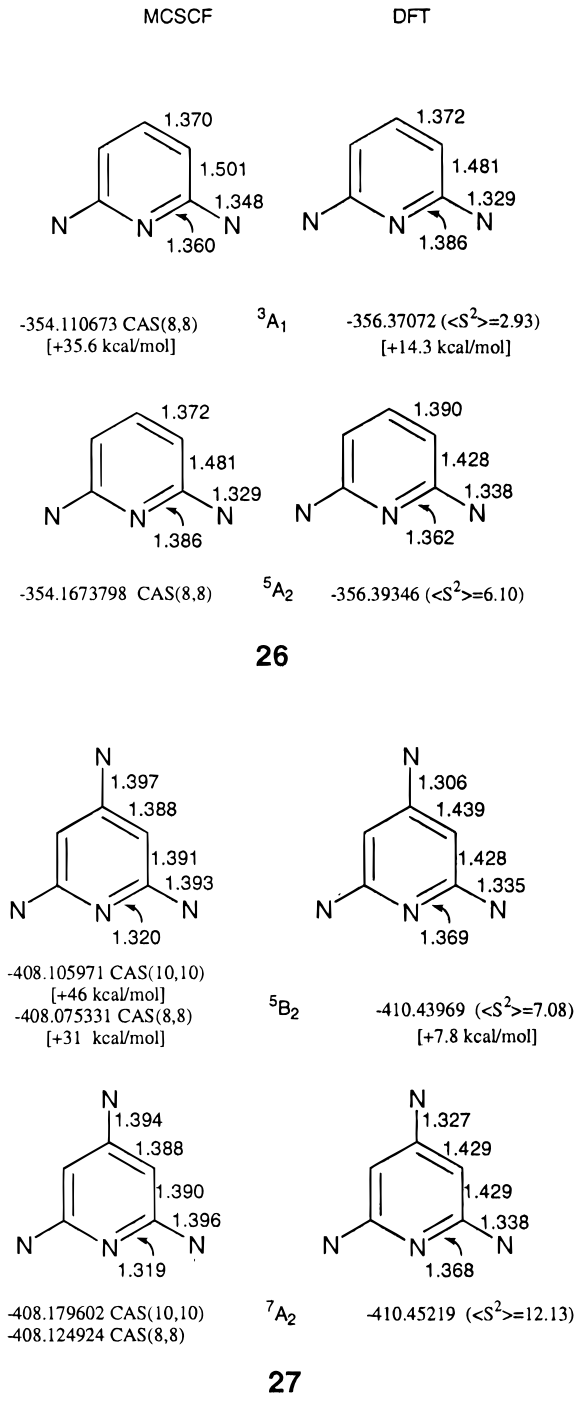

Figure 7. Ab initio and DFT computed energies and selected bonding parameters for model systems **26** and **27**. Values for **26** are from CASSCF(8,8)/6-31G*//CASSCF(8,8)/6-31G* results. Ab initio values for **27** are from CASSCF(10,10)/6-31G*//CASSCF(8,8)/6-31G* and CAS(8,8)/6-31G*//CAS(8,8)/6-31G* results. All DFT results are obtained using Gaussian 98 with B3LYP/6-31G*, using GUESS(MIX) keyword for excited states of lower multiplicity than septet. Energies are given in hartrees and bond lengths in angstroms. The high-spin to low-spin energy gap for each molecule is given in brackets, [ ]; a positive number means that the high-spin state is lower. $\langle S^2 \rangle$ is the spin-squared expectation value.

(22) (a) Schmidt, M. M.; Baldridge, K. K.; Boatz, J. A.; Jensen, J. H.; Koseki, S.; Gordon, M. S.; Nguyen, K. A.; Windus, T. L.; Elbert, S. T. *QCPE Bull.* **1990**, *10*, 52. (b) Schmidt, M. W.; Baldridge, K. K.; Boatz, J. A.; Elbert, S. T.; Gordon, M. S.; Jensen, J. H.; Koseki, S.; Matsunaga, N.; Nguyen, K. A.; Su, S.; Windus, T. L.; Dupuis, M.; Montgomery, J. A. *J. Comput. Chem.* **1993**, *14*, 1347−1363.

(23) Frisch, M. J.; Trucks, G. W.; Schlegel, H. B.; Gill, P. M. W.; Johnson, B. G.; Robb, M. A.; Cheeseman, J. R.; Keith, T.; Petersson, G. A.; Montgomery, J. A.; Raghavachari, K.; Al-Laham, M. A.; Zakrzewski, V. G.; Ortiz, J. V.; Foresman, J. B.; Cioslowski, J.; Stefanov, B. B.; Nanayakkara, A.; Challacombe, M.; Peng, C. Y.; Ayala, P. Y.; Chen, W.; Wong, M. W.; Andres, J. L.; Replogle, E. S.; Gomperts, R.; Martin, R. L.; Fox, D. J.; Binkley, J. S.; Defrees, D. J.; Baker, J.; Stewart, J. P.; Head-Gordon, M.; Gonzalez, C.; Pople, J. A.; Gaussian Inc.: Pittsburgh, PA, 1998.

(24) (a) Becke, A. D. *Phys. Rev. A* **1988**, *38*, 3098−3100. (b) Lee, C.; Yang, W.; Parr, R. G. *Phys. Rev. B* **1988**, *37*, 785−789.

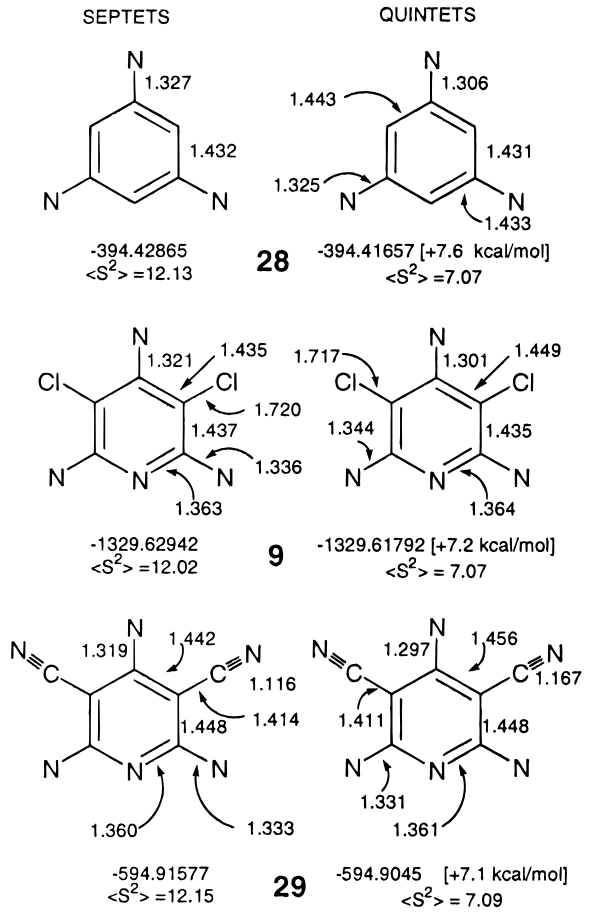

Figure 8. Density functional results for states of trinitrenes **9**, **28**, and **29**. Septet states were done with the UB3LYP/6-31G* method, quintet and triplet states with the B3LYP/6-31G* GUESS(MIX) keyword set in Gaussian 98. Energies are given in hartrees and bond lengths in angstroms. The high-spin to low-spin energy gap for each molecule is given in brackets, [ ]; a positive number means that the high-spin state is lower. $\langle S^2 \rangle$ is the spin-squared expectation value.

The DFT results for trinitrene **27** were analogous to those for dinitrene **26**, in that the predicted septet−quintet energy gap is smaller than predicted by the CASSCF methodology: 8 kcal/mol vs about 25 kcal/mol. The DFT results show strong spin contamination of the excited quintet states, which may result in artifactual lowering of the septet−quintet gap. Regardless of the method, the parity-derived preference for a high-spin state is strong in this system, arguing against the possibility that the various states of different multiplicity in the 2,4,6-pyridinetrinitrenes are nearly degenerate.

Finally, we were concerned whether the heteroatom substitution effects might alter the parity-based ground-state multiplicities of dichloro trinitrene **9** or the putative dicyano trinitrene **29**. Since DFT computations gave the smallest septet to quintet energy gaps in the unsubstituted model system **27**, they were considered the best for qualitative ground state prediction, in that a computational high-spin prediction seems likely to be experimentally realized. DFT geometries and energies of the septet and quintet states of **9** and **29** are given in Figure 8, with a comparison to phenyl-1,3,5-trinitrene (**28**). In all cases, the septet state is predicted to be the ground state by about 7 kcal/mol, despite different substitution patterns. The quintet wave functions are substantially spin contaminated, with spin-squared expectation values of about seven, whereas a pure quintet should have a value of six. This may actually lead to an underestimation of the septet to quintet gap. Since substantial septet preference is seen in these cases, we presume this to be the experimental fact, in accord with the Curie plot observations. This is not a certainty due to the inherent limitations of Curie law experiments[20] but parity theory analysis, computation, and experiment all support septet ground states.

The Order of Azide Photocleavages. Irradiation of compound **1** in frozen 2-MeTHF at 77 K for 3 min at 335 nm gave predominantly the low-field mononitrene peak for **5** and the high-field 2,6-dinitrene peak for **8**, analogous to those observed in Figure 2a. Much smaller intensity peaks were observed that were attributable to high-field mononitrene **6** and quintet 2,4-dinitrene **7**. The peaks attributable to trinitrene **9** were too small to observe clearly, if present. In combination with spectral evidence described in the preceding article by Wentrup and coworkers,[18] this result shows that the azido groups at the 2,6-positions in **1** are preferentially cleaved to give 2-nitrenopyridine (**5**) and 2,6-dinitrenopyridine (**8**). Minor additional amounts of 4-azido photocleavage lead to mononitrene **6** and dinitrene **7**.

Samples that were enriched in 2-nitreno and 2,6-dinitreno pyridines due to lower energy photolysis could be subjected to subsequent, broadband irradiation through a Pyrex filter, and the spectrum in Figure 2a was again obtained. Thus, it seems clear that there is a preference for 2-azide photocleavage in these systems, when substituent effects such as those in dicyano **3** do not interfere. Overall, when mild photolysis conditions are used, 2,6-dinitrene and 2-nitrene products predominate, although there is minor formation of products associated with 4-nitrene formation. The difference in spectral appearances as a function of irradiation conditions suggests that 2-azido and 4-azido photocleavages compete, but a more thorough investigation of ESR active photoproducts as functions of irradiation time and wavelength would be required to quantitative this observation.

Summary. The cryogenic matrix photolysis of 3,5-disubstituted 2,4,6-triazidopyridines shows varying behavior as a function of substitution. Triplet mononitrene, quintet dinitrene, and septet dinitrene species are formed in varying amounts from differently substituted precursors. The strongly electron-withdrawing cyano substituent hinders the formation of nitrenes in these systems. The arene nitrogen atom on the pyridine ring perturbs electron density on the nitrenes at the ortho position relative to that in the para position, leading to an unusually large quintet zero field splitting for the 2,6-pyridine dinitrenes. Computational modeling predicts that 2,6-pyridyl dinitrenes and 2,4,6-pyridyl trinitrenes have high-spin ground states with sizable quintet−triplet energy gaps; experimental evidence is consistent with these predictions. Simulation of the high-spin quintet and septet ESR spectra is very useful to assist with the assignment of high-spin spectral peaks that have hitherto not been identified. Future studies should find the present assignment of 2,6-pyridyl dinitrene quintet spectral peaks to be useful, as well as the assignment of the novel septet trinitrene ESR peaks. These septet trinitrenes have perhaps the largest number of unpaired spins per atom among organic open shell species identified to date (only the report by Wasserman et al.[16] has described the spectral detection of another molecule with three nitrene units on a single aryl ring). The overall results support use of qualitative spin parity rules for predicting spin multiplicity in conjugated polynitrenes, even when heteroatom electronic perturbation is likely.

Experimental Procedures

3,5-Dichloro-2,4,6-triazidopyridine (1). A solution of 2.5 g (10 mmol) of pentachloropyridine and 2.6 g (40 mmol) of sodium azide in 200 mL of 10% aqueous acetone was heated at 70 °C for 72 h. Acetone

was removed under reduced pressure and 200 mL of ice water was added to the residue. The white solid was filtered off, dried at room temperature under vacuum, and recrystallized from ethanol to give 2.6 g (94% yield) of 2,4,6-triazido-3,5-dichloropyridine with mp 78−79 °C. IR (cm^{-1}, KBr): 2164s, 2138s, 2127s, 2085w (N_3), 1575m, 1557m, 1533m, 1375vs, 1275w, 1255m, 1211w, 1163w, 1109w, 932w, 836w, 771w, 740w, 732w, 536w. UV−vis (MeOH; λ_{max}/nm(ϵ)): 333 (7800), 272 shoulder (17300), 252 (37900). ^{13}C NMR (100.62 MHz,$CDCl_3$, δ): 148.67 (C-2, C-6),144.57 (C-4), 109.14 (C-3, C-5). Anal. Calcd for $C_5N_{10}Cl_2$: C 22.16, N 51.68. Found: C 22.24, N 51.61. Mass spectrum (*m*/*z*, %): 270 (43.3%, parent $C_5N_{10}Cl_2$), 242 (2.0%, M−N_2), 228 (1.6%, M−N_3), 87 (100%, C_2N_2Cl).

3-Chloro-5-cyano-2,4,6-triazidopyridine (**2**). The synthesis and characterization of compound **2** are described elsewhere.[7]

3,5-Dicyano-2,4,6-triazidopyridine (3). The synthesis and characterization of compound **3** are described elsewhere.[8]

3,5-Difluoro-2,4,6-triazidopyridine (4). The synthesis and characterization of compound **4** are described elsewhere.[9]

Photolysis and ESR Spectroscopy. Previously described compounds were checked by ^{13}C NMR spectroscopy and FAB mass spectrometry before use in ESR experiments. All samples were stored wrapped in aluminum foil in a refrigerator to minimize photodecomposition by room light. Under these conditions, compounds **1**−**4** appear to be stable for many months, perhaps indefinitely.

For typical ESR spectral experiments, an appropriate sample of triazide precursor was dissolved in 2-methyltetrahydrofuran (MeTHF) in a 4 mm o.d. quartz sample tube, subjected to a 3-fold freeze−pump−thaw degassing procedure and sealed under vacuum, frozen at 77 K, and photolyzed for 2−5 min with a 1000 W xenon arc lamp at >300 nm (Pyrex-filter) at a distance of about 5 cm. The sample was rapidly transferred to a Suprasil II vacuum-jacketed finger dewar that was placed into the cavity of a Bruker ESP-300 spectrometer equipped with a standard Bruker computerized multiscan acquisition interface. Most spectra were obtained over a 100−9900 G (G) region at a modulation frequency of 100.0 kHz and a microwave power setting of 20 dB. Microwave frequencies were determined using a Hewlett-Packard 5350B frequency counter. Variable-temperature analysis was carried out using an Oxford Instruments ESR-900 liquid helium cryostat, with temperature calibration carried out using carbon electrodes.

Acknowledgment. Financial support of this work by the National Science Foundation (NSF CHE-9521594 and CHE-9740401) is gratefully acknowledged. Additional support for computational resources was provided by the University of Massachusetts. We thank Prof. K. Sato for communicating results from a recent investigation[4] of triazido-*s*-triazine photochemistry and Prof. C. Wentrup for helpful discussions and advance sharing of the results described in the preceding article.[18] We thank Prof. Sato for making available to us the eigenfield ESR simulation program described in his thesis.[11f]

Supporting Information Available: Molecular orbital contour diagrams generated using the program MOLDEN[25] to visualize output from GAMESS,[22] Figure S1 of DFT Mulliken spin density results for septet states of **9** and **27**−**29**, and a summary of the archival output for various CASSCF and DFT computations for **9** and **26**−**29** (16 pages). This material is available free of charge via the Internet at http://pubs.acs.org.

JA993131C

(25) Schaftenaar, G. Program MOLDEN, version 3.4 for Silicon Graphics workstation; see http://www.caos.kun.nl/~schaft/molden/molden.html; "MOLDEN, a visualization program of molecular and electronic structure", 1991, CAOS/CAMM Center.